

β -Gallium Oxide Devices: Progress and Outlook

Masataka Higashiwaki

Beta-gallium oxide (β -Ga₂O₃) has a history of research and development for over 70 years; however, it has attracted little attention as a semiconductor material for a long time. The situation has drastically changed in the past decade, and research on its material properties and developments of growth and device technologies has become active worldwide, mainly from expectations for applications to next-generation power devices. Most of the specific material properties are attributed to its extremely large bandgap energy of 4.5 eV. The other important material feature is that large-size single-crystal bulks can be synthesized by melt growth methods. Herein, after introducing the material properties of β -Ga₂O₃ that are important for electronic devices, the current status of bulk melt growth and epitaxial thin-film growth technologies is given. State-of-the-art β -Ga₂O₃ diodes and transistors are also discussed, including future prospects.

1. Introduction

What pops into your mind when you hear a name of gallium oxide (Ga₂O₃)? For some readers, it would be a bitter memory on the development of GaAs metal–oxide–semiconductor field-effect transistors (MOSFETs). The existence of Ga₂O₃ as a material has been widely known; however, it used to be recognized as a poor-quality gate dielectric for GaAs FETs, providing high-density interface states and defects. In fact, research and development (R&D) on Ga₂O₃ as a semiconductor material has a long history for more than 70 years;^[1,2] however, Ga₂O₃ had attracted little attention from the semiconductor community for a long time. The position of Ga₂O₃ has totally changed now; interest in Ga₂O₃ grew in the 2010s, and it has acquired wide recognition as a new type of semiconductor.

Although several polymorphs exist for Ga₂O₃, the most stable β -phase and the other metastable phases, herein, discussions focusing on β -Ga₂O₃ are given.

2. Material Properties of β -Ga₂O₃

Comparisons of important material parameters for applications in transistors and diodes between β -Ga₂O₃ and the other major

semiconductors are shown in Table 1. Each parameter is illustrated in detail in the following subsections.

2.1. Breakdown Electric Field

Currently, R&D on Ga₂O₃ FETs and Schottky barrier diodes (SBDs) is mostly aiming for applications in next-generation power devices. This can be attributed to two distinguished features in terms of material properties: 1) the extremely large bandgap energy (E_g) of 4.5 eV^[3] and 2) the high breakdown electric field (E_{br}) resulting from E_g .^[4] When designing vertical power devices with the same breakdown voltage (V_{br}), using materials with a large E_{br} , it is possible to decrease the thickness of the drift

layer sustaining an applied voltage and/or increase doping concentration in it. Note that the intrinsic E_{br} of β -Ga₂O₃ limited by the avalanche breakdown event has never been experimentally estimated. This is because breakdown events of Ga₂O₃ FETs and SBDs have been caused by permanent destruction due to concentration of the electric field at the edges of gate and anode electrodes, respectively. The maximum E_{br} reported so far is 7 MV cm⁻¹, which was extracted from V_{br} given by permanent device failure.^[5] For β -Ga₂O₃, it has been expected from theoretical calculation that the avalanche E_{br} would be over 8 MV cm⁻¹.^[6]

2.2. Room-Temperature Electron Mobility

The maximum electron mobility (μ) in β -Ga₂O₃ at room temperature (RT) has been theoretically predicted to be ≈ 200 cm² V⁻¹ s⁻¹, which is limited by the longitudinal optical phonon scattering with relatively small energies of around 40 meV.^[7,8] In fact, the highest electron μ experimentally observed until now was 180 cm² V⁻¹ s⁻¹.


2.3. Saturation Electron Velocity

The saturation electron velocity (V_{sat}), which is the other important parameter for carrier transport, has been theoretically calculated to be $1.0\text{--}1.5 \times 10^7$ cm s⁻¹.^[9] This value is comparable with that of Si and about half of those of SiC and GaN, implying that Ga₂O₃ FETs are applicable for high-frequency wireless communications.

2.4. n-Type Doping

As donor dopants to form n-Ga₂O₃, group IV species such as Si, tin (Sn), and germanium (Ge) have been commonly used. They form

M. Higashiwaki
Advanced ICT Research Institute
National Institute of Information and Communications Technology
Koganei, Tokyo 184-8795, Japan
E-mail: mhigashi@nict.go.jp

 The ORCID identification number(s) for the author(s) of this article can be found under <https://doi.org/10.1002/pssr.202100357>.

DOI: 10.1002/pssr.202100357

Table 1. Comparisons of material properties between major semiconductors and β -Ga₂O₃.

	Si	GaAs	4 H-SiC	GaN	β -Ga ₂ O ₃
Bandgap E_g [eV]	1.1	1.4	3.3	3.4	4.5
Relative dielectric constant ϵ	11.8	12.9	9.7	9.0	10.2–12.4
Breakdown electric field E_{br} [MV cm ⁻¹]	0.3	0.4	2.5	3.3	>7
Room-temperature electron mobility μ [cm ² V ⁻¹ s ⁻¹]	1400	8000	1000	1200	≈200
Saturation electron velocity V_{sat} [$\times 10^7$ cm s ⁻¹]	1.0	2.0	2.0	2.5	1.0–1.5
Thermal conductivity [W cm ⁻¹ K ⁻¹]	1.5	0.55	2.7	2.1	0.11–0.27
Baliga's FOM ($= \epsilon \mu E_{br}^3$)	1	15	340	870	1570–1900
Johnson's FOM ($= E_{br}^2 V_{sat}^2$)	1	7	280	760	540–1200

shallow donor states in Ga₂O₃,^[10,11] and their activation ratios are quite high. Precise control of electron density (n) in the wide range of 10^{15} to 10^{20} cm⁻³ has been achieved by intentional donor doping.

2.5. p-Type Doping

In contrast to n-type doping, p-type doping of β -Ga₂O₃ is quite difficult, as is the case with other oxide semiconductors. This is due to the following three physical reasons. 1) Oxygen (O) ions are almost localized in β -Ga₂O₃, because the valence band is formed by O 2p orbitals having very strong bonding. Actually, theoretical calculations revealed that activation energies of all the acceptor candidates such as magnesium (Mg), zinc (Zn), beryllium (Be), and nitrogen (N) become at least larger than 1 eV.^[12,13] 2) The valence band top of Ga₂O₃ is almost flat, leading to a very large hole effective mass.^[14–16] In consequence, it is difficult to have sufficient hole conductivity in both cases of low-field drift and diffusion. 3) Self-trapping of free holes was expected to occur in Ga₂O₃ due to local lattice distortion.^[17] This effect should be one of the factors to take hole conductivity away. All the three issues have to be resolved to obtain hole-conductive p-Ga₂O₃; the author considers that it is nearly impossible.

2.6. Thermal Conductivity

Thermal conductivity is one of the important parameters to suppress degradation of device performance caused by an increase in channel temperature at the on-state. Like other oxide materials, Ga₂O₃ has low thermal conductivity, which is 1/6 that of Si and less than 1/10 those of SiC and GaN.^[18,19] Heat generation under high-power operation is inevitable even in high-efficiency power devices, and the device performance strongly depends on its heat dissipation capacity, as a drift layer resistance increases with increasing operation temperature due to a decrease in electron μ . Therefore, low thermal conductivity is a serious potential weakness of Ga₂O₃, and thermal management is one of the most important technical challenges.

2.7. Device Figure of Merit

Baliga's figure of merit (BFOM) has been the most common parameter to see how suitable a material is for power-switching devices.^[20,21] It can be calculated using the material parameters

shown in Table 1, and the BFOM of β -Ga₂O₃ is several times larger than those of SiC and GaN. This is because it is proportional to the cube of E_{br} but only linearly proportional to μ as the definitional identity. For device structures designed to have the same V_{br} , β -Ga₂O₃ devices are expected to provide a smaller on-resistance (R_{on}), that is, a lower conduction loss than those of the other semiconductor devices.

Johnson's FOM (JFOM) is often used to evaluate material potential for applications in high-frequency power amplifiers.^[22] The β -Ga₂O₃ JFOM is comparable with that of GaN. However, in case of radio-frequency (RF) FETs, the actual power-added efficiency is at the level a little larger than 50%, that is, the other half is converted to heat. Therefore, it can be considered that the poor heat dissipation of Ga₂O₃ devices that originated from its low thermal conductivity becomes a severe issue especially for applications in RF power amplifiers.

3. Bulk Melt Growth of β -Ga₂O₃

It is possible to synthesize β -Ga₂O₃ single-crystal bulks by several melt growth methods; this feature is a strong advantage over SiC and GaN. There have been many reports on its bulk synthesis by various melt growth methods such as Verneuil,^[23] floating zone,^[24,25] Czochralski (CZ),^[26,27] edge-defined film-fed growth (EFG),^[25,28] and Bridgman.^[29] Now, Ga₂O₃ wafers produced from CZ and EFG bulks are commercially available. The size of the wafers produced from CZ bulks remains to be up to 2 in. diameter.^[26,27] In contrast, EFG Ga₂O₃ wafers have been developed up to 6 in. diameter in R&D and commercially produced up to 4 in. diameter. Therefore, in the present stage, EFG is a step ahead of CZ as the Ga₂O₃ wafer production technology. Ga₂O₃ wafers have been of high quality for device applications, represented by a low dislocation density of less than 10^4 cm⁻². Furthermore, it can be expected that availability of melt growth methods to synthesize single-crystal Ga₂O₃ bulks leads to low-cost wafer mass production in the future.

4. Epitaxial Thin-Film Growth of β -Ga₂O₃

4.1. Molecular Beam Epitaxy

As was the case with other compound semiconductors, even in Ga₂O₃, molecular beam epitaxy (MBE) preceded other epitaxial

growth technologies at the early stage of R&D. Conventional gas-source MBE machines are used for Ga₂O₃ growth. Ga molecular beam supplied from a Knudsen cell is used as Ga source. In contrast, there are two types of O sources: ozone (O₃) and O radicals produced by decomposition of O₂ gas using an RF plasma cell. The MBE of Ga₂O₃ and other oxide semiconductors has unique growth kinetics ruled by volatile suboxides.^[30,31]

Currently, MBE-grown Ga₂O₃ thin films are often utilized for lateral FET development. Each O source has its own advantages and disadvantages; however, both techniques can provide sufficiently high-quality materials for lateral FETs.^[32–34] Furthermore, (AlGa)₂O₃/Ga₂O₃ modulation-doped structures and formation of 2D electron gas at the interface have been demonstrated through the use of MBE-grown epitaxial wafers.^[35,36]

4.2. Halide Vapor Phase Epitaxy

Ga₂O₃ thin-film epitaxial growth technology using halide vapor phase epitaxy (HVPE) was developed in 2014.^[37] GaCl and O₂ are typically used as Ga and O sources, respectively. The growth rate of Ga₂O₃ thin films can be increased up to 20 μm h^{−1} without any degradation of crystal quality. The residual *n* of unintentionally doped (UID) Ga₂O₃ (001) films is very low, which is less than 1 × 10¹³ cm^{−3}.^[38] Si doping conducted by simultaneous supply of SiCl₄ during Ga₂O₃ growth can provide accurate control of *n* in the wide range from 10¹⁵ to 10¹⁹ cm^{−3}.^[39] The maximum electron *μ* at RT reported so far is ≈150 cm² V s^{−1}. Epitaxial wafers with HVPE-grown n-Ga₂O₃ layers have been widely used for the development of vertical diodes and FETs in recent years.

4.3. Metal–Organic Chemical Vapor Deposition

Ga₂O₃ metal–organic chemical vapor deposition (MOCVD) technology has been used for a long time; however, it used to be inferior to MBE and MOCVD in terms of crystal quality and growth rate. The progress has become remarkable in the past few years, and the crystal quality of MOCVD-grown Ga₂O₃ films has improved. For instance, the residual *n* of UID Ga₂O₃ films grown by MOCVD decreased to the order of 10¹⁵ cm^{−3}. RT and low-temperature electron *μ* reached 180 and 11 000 cm² V s^{−1}, respectively.^[40–42] These electrical properties are comparable with those of HVPE-grown n-Ga₂O₃ films. Moreover, the growth rate, which used to be very slow at 0.1–0.2 μm h^{−1}, was enhanced to >3 μm h^{−1}.^[43] Ease of epitaxial growth of (AlGa)₂O₃/Ga₂O₃ heterostructures is also an important feature of MOCVD in common with MBE.^[44,45]

5. β-Ga₂O₃ Diodes

5.1. SBDs

There have been many reports on vertical Ga₂O₃ SBD developments for the last 3–4 years. This is because the device structure itself is relatively simple, and high-quality Ga₂O₃ epitaxial wafers grown by HVPE are commercially available.

In the author's group, simple SBD structures with various drift layers having *n* = 10¹⁶–10¹⁷ cm^{−3}, as shown in Figure 1a, were fabricated as a first step of R&D on vertical Ga₂O₃ devices, to characterize crystal quality and electrical properties of HVPE-

grown drift layers.^[46] Temperature-dependent current density–voltage (*J*–*V*) characteristics at forward and reverse voltages of a typical SBD with a drift layer having *n* = 1.2 × 10¹⁶ cm^{−3} are shown in Figure 1b,c, respectively. The on-resistance (*R*_{on}) was 3 mΩ cm², and the reverse *V*_{br} was about 500 V. The forward *J*–*V* characteristics can be reproduced by the textbook thermionic emission model. The ideality factor kept an excellent value of 1.03 ± 0.01 at all the measurement temperatures. In contrast, the reverse *J*–*V* characteristics were well explained by the thermionic field emission model, as is the case with other wide-bandgap semiconductors. These results indicate that it is relatively easy to form high-quality Schottky contacts on HVPE Ga₂O₃ films by use of Pt.

Subsequently, we fabricated Ga₂O₃ SBDs with edge termination structures such as a field plate and a N-ion-implanted guard ring to mitigate electric field concentration at the anode electrode edge.^[47,48] The reverse *V*_{br} of the SBDs was improved to 1,076 and 1,430 V, respectively, with keeping low values of *R*_{on} ≈ 5 mΩ cm². Note that the former was the first demonstration of *V*_{br} > 1 kV for any Ga₂O₃ devices.

As another technique to enhance *V*_{br}, Ga₂O₃ trench SBDs, as shown in Figure 2, were reported from Cornell University.^[49,50] An anode electrode was formed to cover trench sidewalls on which an Al₂O₃ dielectric was deposited. At the reverse-biased off-state condition, the depletion region laterally spread from the sidewalls, leading to an increase in *V*_{br}. A very high *V*_{br} of over 2 kV was demonstrated for the trench SBDs, keeping *R*_{on} ≈ 10 mΩ cm².

5.2. p–n Heterojunction Diodes

A relatively high-quality interface is often obtained between single-crystal and amorphous oxides without any sophisticated process and/or treatment. Using this feature, p–n heterojunction diodes between n-Ga₂O₃ and p-type amorphous oxides such as Cu₂O and NiO have been developed.^[51–53] Good device characteristics with *R*_{on} < 10 mΩ cm² and *V*_{br} > 1 kV were achieved for both the amorphous materials.

5.3. Benchmark

Benchmark *R*_{on}–*V*_{br} performance of the state-of-the-art Ga₂O₃ SBDs^[47–50,54–56] and p–n heterojunction diodes^[51–53] is shown in Figure 3. The characteristics of both types of diodes have already exceeded the Si theoretical limit but never reached those of SiC and GaN. This is because the *V*_{br} of all the Ga₂O₃ diodes was determined by permanent structural failure. Effective edge termination structures are strongly demanded to further improve *V*_{br}, with keeping a low *R*_{on}.

6. β-Ga₂O₃ FETs

6.1. Lateral FETs

The first demonstration of single-crystal Ga₂O₃ FETs, which was accomplished by the author's group, made more people familiar with Ga₂O₃ and became a trigger for its worldwide R&D activities.^[57] Subsequently, we developed elemental process technologies including Si-ion implantation doping^[58] and Al₂O₃ gate

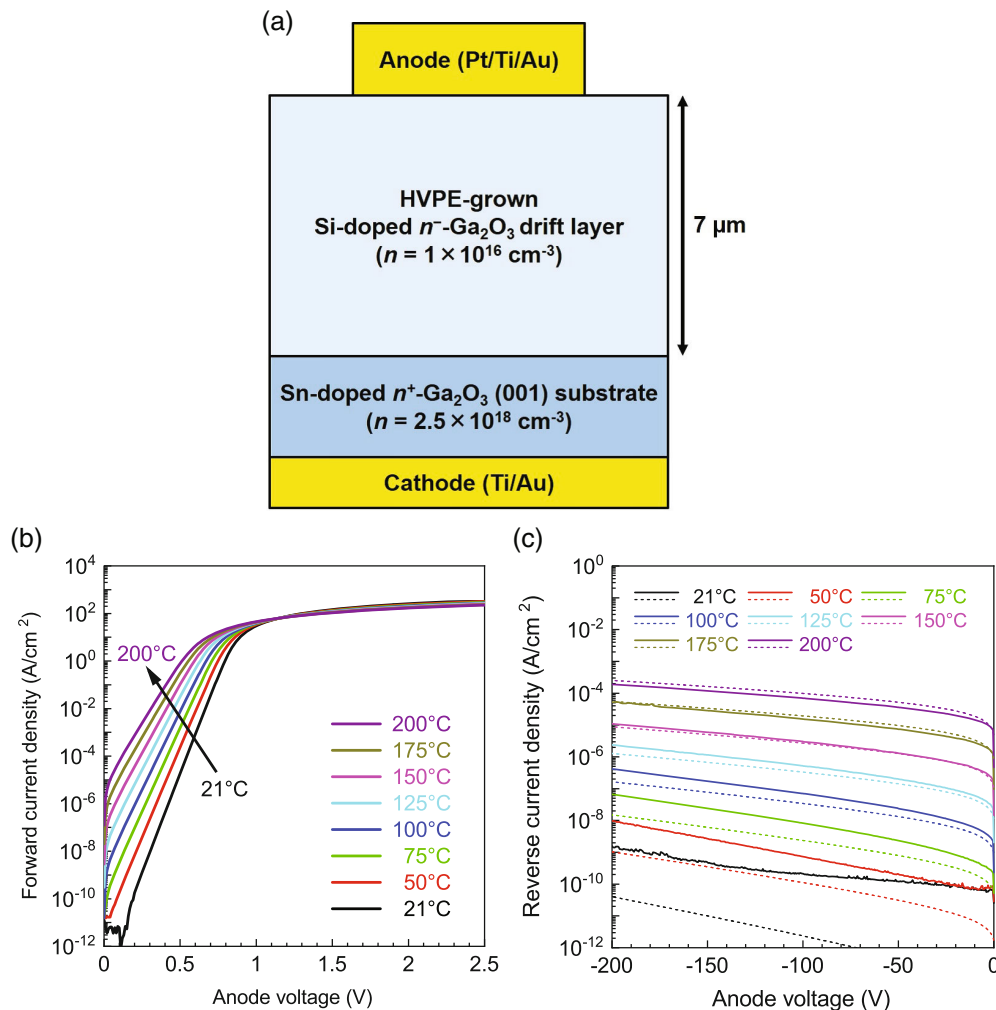


Figure 1. a) Schematic cross section of Ga₂O₃ SBD structure. b,c) Its temperature-dependent forward (b) and reverse (c) *J*-*V* characteristics. a-c) Adapted with permission.^[46] Copyright 2016, American Institute of Physics.

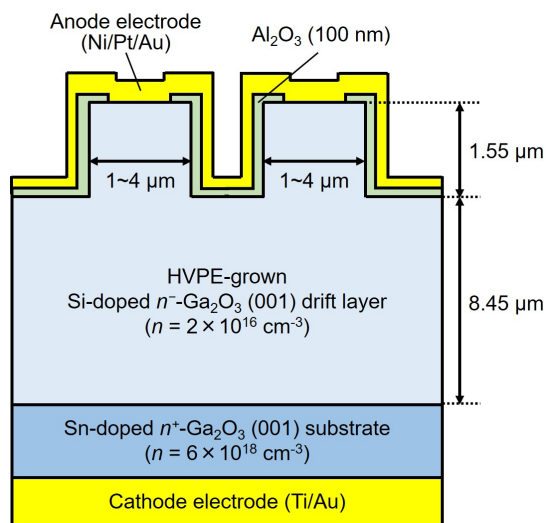


Figure 2. Schematic cross section of Ga₂O₃ trench SBD structure.

dielectrics formed by atomic layer deposition,^[59] and fabricated more advanced FET structures such as depletion-mode MOSFETs^[60,61] and field-plated MOSFETs^[62] (Figure 4) using the newly developed processes.

The lateral Ga₂O₃ FETs were important to develop device process technologies and demonstrate their potential for power electronics applications; however, in practice, there are not many application fields for them. Ga₂O₃ is expected to have high resistance against stresses due to high temperature, radiation, and corrosive gases, as well as being suited for power devices. Hence, it can be considered that Ga₂O₃ FETs have a large potential even for wireless communication and signal processing applications in harsh environments in which it is difficult for existing semiconductor devices to keep operating for a long time.

Based on the idea, we investigated gamma-ray tolerance of the Ga₂O₃ field-plated MOSFETs.^[63] The MOSFETs showed small degradation of DC output characteristics even after high cumulative gamma-ray irradiation dose up to 1.6 MGy. Note that the irradiation dose is at a level of exceeding requirements for typical

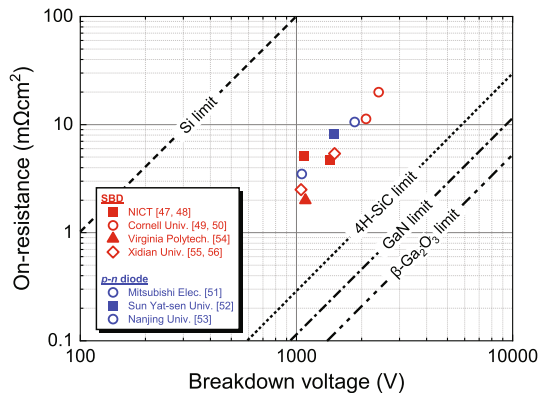


Figure 3. Benchmark plots of Ga_2O_3 SBDs and p-n diodes.

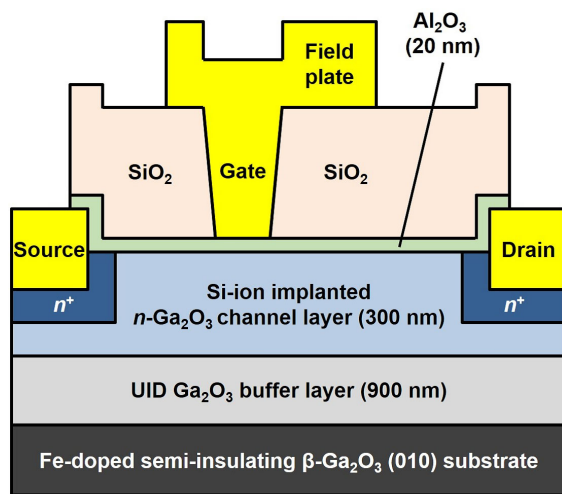


Figure 4. Schematic cross section of lateral Ga_2O_3 field-plated FET structure. Adapted with permission.^[62] Copyright 2016, IEEE.

space applications. Furthermore, stable operation of MOSFETs has been confirmed up to 300°C .^[62] These results indicate a large potential of Ga_2O_3 FETs for applications in high-temperature and/or radiation-hard electronics.

Recently, we developed highly scaled Ga_2O_3 MOSFETs, which aimed for applications in high-frequency wireless communications and logic circuits operating in harsh environments.^[64] The MOSFETs with a gate length (L_g) of 200 nm demonstrated a current-gain cutoff frequency (f_T) of 9 GHz and a maximum oscillation frequency (f_{max}) of 27 GHz, as shown in **Figure 5**. Comparable RF small-signal characteristics have also been reported from other institutes.^[65,66] These RF device characteristics indicate that Ga_2O_3 FETs can be used for wireless communications at frequencies up to ≈ 10 GHz. However, it is also undeniable that the RF device characteristics are inferior to those of GaN FETs with similar structures. The development of high-frequency Ga_2O_3 FETs has just begun and thus should have much room for improvement. Nevertheless, given the fundamental material properties of Ga_2O_3 such as V_{sat} and thermal conductivity, the author considers that Ga_2O_3 FETs cannot rival GaN FETs in performance for broad applications such as base stations and wireless radars in which GaN FETs have already been adopted for use.

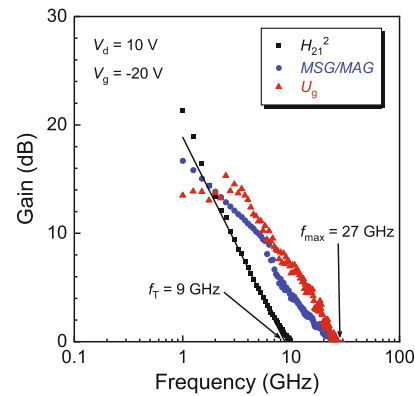


Figure 5. Small-signal RF characteristics of lateral Ga_2O_3 MOSFET ($L_g = 200$ nm). Adapted with permission.^[64] Copyright 2020, American Institute of Physics.

6.2. Vertical FETs

As is generally known, vertical transistors are favorable for high-voltage and high-power device applications; however, the development of vertical Ga_2O_3 FETs has little been implemented yet until now. Here, development examples conducted by the group at Cornell University and the author's group are introduced.

We fabricated vertical Ga_2O_3 MOSFET structures with a current aperture, as shown in **Figure 6**.^[67] Its operation principle is as follows. Vertical electron current flow from the source to the drain is restricted only in the aperture part. The gate electrode, which is located immediately above the aperture, controls the drain current by means of a gate depletion layer. Most of the process technologies to fabricate the vertical MOSFETs were the same as those developed for the lateral MOSFETs. The only new portion was a buried p- Ga_2O_3 current blocking layer (CBL) formed in an n- Ga_2O_3 drift layer by N-ion-implantation doping.^[68] As mentioned in Section 2.5, N acts as a deep acceptor in Ga_2O_3 , and it is impossible to obtain p- Ga_2O_3 with sufficient hole conductivity. However, the deep acceptor states can pin the Fermi level, resulting in the formation of a large energy barrier of about 3 eV at the p-n junction.

The current-aperture vertical Ga_2O_3 MOSFETs were fabricated using ion-implantation doping processes that have been widely used for mass production of vertical Si and SiC power devices. In the fabrication, we used three ion-implantation processes in total to form p- Ga_2O_3 current blocking, n- Ga_2O_3 channel, and n⁺- Ga_2O_3 ohmic contact layers. Depletion-mode vertical MOSFETs showed reasonably good device characteristics including a maximum I_d of 0.4 kA cm^{-2} , an R_{on} of $32 \text{ m}\Omega \text{ cm}^2$, and an I_d on/off ratio of over eight orders of magnitude (**Figure 7a,b**). Normally off operation was also achieved by decreasing n of the n- Ga_2O_3 channel region from 1.5×10^{18} to $5 \times 10^{17} \text{ cm}^{-3}$.^[69] The maximum V_{br} still remained at a low value of 260 V, which was due to the low quality of the CBL; therefore, the process condition of the N-ion-implantation doping should be further improved.

Vertical fin-channel Ga_2O_3 FETs were reported from the same group at Cornell University that developed trench SBDs.^[70] Normally off operation was achieved for enhancement-mode

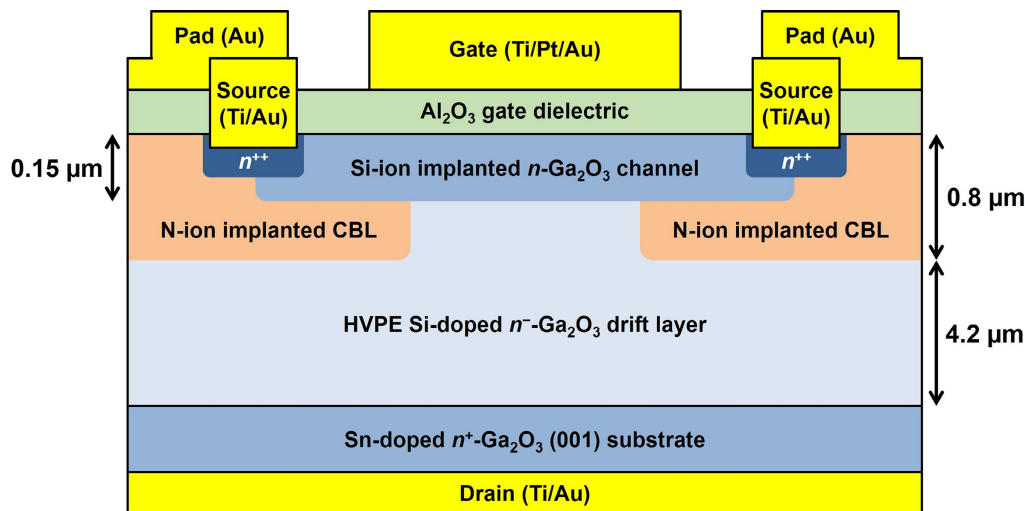


Figure 6. Schematic cross section of vertical current-aperture Ga_2O_3 MOSFET structure. Adapted with permission.^[67] Copyright 2019, IEEE.

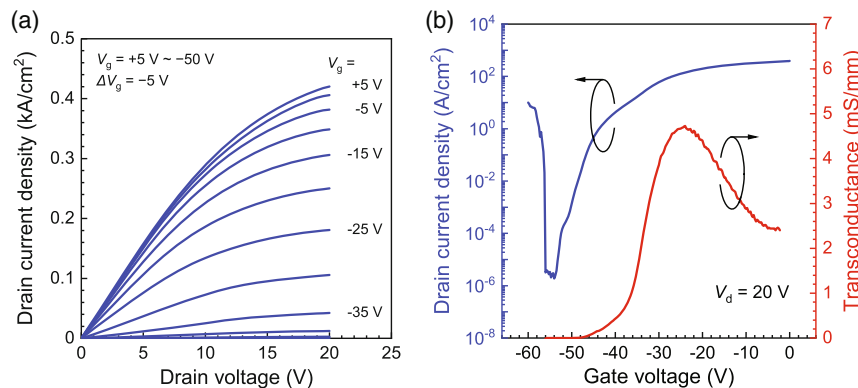


Figure 7. a) DC I_d - V_d output characteristics and b) transfer characteristics of vertical D-mode current-aperture Ga_2O_3 MOSFET. a,b) Adapted with permission.^[67] Copyright 2019, IEEE.

FETs with a sub-micrometer fin channel patterned by electron beam lithography. The fin FETs also demonstrated excellent device characteristics such as a maximum I_d of 1 kA cm^{-2} , an R_{on} of $25 \text{ m}\Omega \text{ cm}^2$, an I_d on/off ratio of $>10^8$, and a V_{br} of 2.66 kV. Fin FET structures would be suitable for Ga_2O_3 from its fundamental physical property that normal p-type is unavailable.

7. Conclusion

$\beta\text{-Ga}_2\text{O}_3$ devices possess large potential based on the extremely large bandgap, the high E_{br} , and the availability of melt-grown bulk wafers. However, there is also restriction on designing device structures due to a lack of hole-conductive p-type material. Furthermore, the low thermal conductivity, which directly affects the heat dissipation capacity of devices, is also a severe issue for high-power device applications.

Ten years have passed since the first Ga_2O_3 FET demonstration. It is gratifying that Ga_2O_3 has gained a lot of popularity in

the past ten years and is now largely accepted in the semiconductor community. In contrast, academic institutions make up the vast majority of Ga_2O_3 R&D; it has been less popular in the industry. It is difficult to accelerate the development of Ga_2O_3 devices without active involvements of companies, which will actually produce and sell Ga_2O_3 -based devices and components. Even from the worldwide trend, it is obvious that highly efficient power-switching devices become key in energy saving. Harsh environment electronics that leads to extending applications fields of semiconductor devices should be demanded. From the current situation, it remains to be seen whether Ga_2O_3 ends up with a popular material in academic societies for a short while or becomes one of the fundamental semiconductors like Si, GaAs, and GaN; reaching industrialization depends on the next ten years.

Acknowledgements

Part of the work introduced here was supported by Council for Science, Technology and Innovation (CSTI), Cross-ministerial Strategic

Innovation Promotion Program (SIP), "Next generation power electronics" (funding agency: New Energy and Industrial Technology Development Organization), and the Strategic Information and Communications R&D Promotion Program (SCOPE) of the Ministry of Internal Affairs and Communications, Japan. The author would like to express deepest appreciation to co-workers and external collaborators for their tremendous contributions in the presented research and development.

Conflict of Interest

The author declare no conflict of interest.

Keywords

field-effect transistors, gallium oxide, Schottky barrier diodes

Received: July 1, 2021

Revised: August 3, 2021

Published online: October 4, 2021

- [1] R. Roy, V. G. Hill, E. F. Osborn, *J. Am. Chem. Soc.* **1952**, 74, 719.
- [2] H. H. Tappin, *Phys. Rev.* **1965**, 140, A316.
- [3] T. Onuma, S. Saito, K. Sasaki, T. Masui, T. Yamaguchi, T. Honda, M. Higashiwaki, *Jpn. J. Appl. Phys.* **2015**, 54, 112601.
- [4] M. Higashiwaki, G. H. Jessen, *Appl. Phys. Lett.* **2018**, 112, 060401.
- [5] Z. Xia, H. Chandrasekar, W. Moore, C. Wang, A. J. Lee, J. McGlone, N. K. Kalarickal, A. Arehart, S. Ringel, F. Yang, S. Rajan, *Appl. Phys. Lett.* **2019**, 115, 252104.
- [6] K. Ghosh, U. Singiseti, *J. Appl. Phys.* **2018**, 124, 085707.
- [7] N. Ma, N. Tanen, A. Verma, Z. Guo, T. Luo, H. Xing, D. Jena, *Appl. Phys. Lett.* **2016**, 109, 212101.
- [8] T. Onuma, S. Saito, K. Sasaki, K. Goto, T. Masui, T. Yamaguchi, T. Honda, A. Kuramata, M. Higashiwaki, *Appl. Phys. Lett.* **2016**, 108, 101904.
- [9] K. Ghosh, U. Singiseti, *J. Appl. Phys.* **2017**, 122, 035702.
- [10] T. Oishi, K. Harada, Y. Koga, M. Kasu, *Jpn. J. Appl. Phys.* **2016**, 55, 030305.
- [11] A. T. Neal, S. Mou, S. Rafique, H. Zhao, E. Ahmadi, J. S. Speck, K. T. Stevens, J. D. Blevins, D. B. Thomson, N. Moser, K. D. Chabak, G. H. Jessen, *Appl. Phys. Lett.* **2018**, 113, 062101.
- [12] J. L. Lyons, *Semicond. Sci. Technol.* **2018**, 33, 05LT02.
- [13] H. Peelaers, J. L. Lyons, J. B. Varley, C. G. Van de Walle, *APL Mater.* **2019**, 7, 022519.
- [14] H. He, R. Orlando, M. A. Blanco, R. Pandey, E. Amzallag, I. Baraille, M. Rérat, *Phys. Rev. B* **2006**, 74, 195123.
- [15] J. B. Varley, J. R. Weber, A. Janotti, C. G. Van de Walle, *Appl. Phys. Lett.* **2010**, 97, 142106.
- [16] H. Peelaers, C. G. Van de Walle, *Phys. Status Solidi B* **2015**, 252, 828.
- [17] J. B. Varley, A. Janotti, C. Franchini, C. G. Van de Walle, *Phys. Rev. B* **2012**, 85, 081109(R).
- [18] M. Handwerg, R. Mitdank, Z. Galazka, S. F. Fischer, *Semicond. Sci. Technol.* **2015**, 30, 024006.
- [19] Z. Guo, A. Verma, X. Wu, F. Sun, A. Hickman, T. Masui, A. Kuramata, M. Higashiwaki, D. Jena, T. Luo, *Appl. Phys. Lett.* **2015**, 106, 111909.
- [20] B. J. Baliga, *J. Appl. Phys.* **1982**, 53, 1759.
- [21] B. J. Baliga, *IEEE Electron Device Lett.* **1989**, 10, 455.
- [22] E. O. Johnson, *RCA Rev.* **1965**, 26, 163.
- [23] A. B. Chase, *J. Am. Ceram. Soc.* **1964**, 47, 470.
- [24] E. G. Villora, K. Shimamura, Y. Yoshikawa, K. Aoki, N. Ichinose, *J. Cryst. Growth* **2004**, 270, 420.
- [25] A. Kuramata, K. Koshi, S. Watanabe, Y. Yamaoka, T. Masui, S. Yamakoshi, *Jpn. J. Appl. Phys.* **2016**, 55, 1202A2.
- [26] Z. Galazka, R. Uecker, D. Klimm, K. Irmischer, M. Naumann, M. Pietsch, A. Kwasniewski, R. Bertram, S. Ganschow, M. Bickermann, *ECS J. Solid State Sci. Technol.* **2017**, 6, Q3007.
- [27] J. D. Blevins, K. Stevens, A. Lindsey, G. Foundos, L. Sande, *IEEE Trans. Semicond. Manuf.* **2019**, 32, 466.
- [28] H. Aida, K. Nishiguchi, H. Takeda, N. Aota, K. Sunakawa, Y. Yaguchi, *Jpn. J. Appl. Phys.* **2008**, 47, 8506.
- [29] K. Hoshikawa, T. Kobayashi, E. Ohba, T. Kobayashi, *J. Cryst. Growth* **2020**, 546, 125778.
- [30] P. Vogt, O. Bierwagen, *Appl. Phys. Lett.* **2015**, 106, 081910.
- [31] P. Vogt, O. Bierwagen, *Appl. Phys. Lett.* **2016**, 108, 072101.
- [32] K. Sasaki, A. Kuramata, T. Masui, E. G. Villora, K. Shimamura, S. Yamakoshi, *Appl. Phys. Express* **2012**, 5, 035502.
- [33] H. Okumura, M. Kita, K. Sasaki, A. Kuramata, M. Higashiwaki, J. S. Speck, *Appl. Phys. Express* **2014**, 7, 095501.
- [34] S. W. Kaun, F. Wu, J. S. Speck, *J. Vac. Sci. Technol. A* **2015**, 33, 041508.
- [35] E. Ahmadi, O. S. Koksaldi, X. Zheng, T. Mates, Y. Oshima, U. K. Mishra, J. S. Speck, *Appl. Phys. Express* **2015**, 10, 071101.
- [36] S. Krishnamoorthy, Z. Xia, C. Joishi, Y. Zhang, J. McGlone, J. Johnson, M. Brenner, A. R. Arehart, J. Hwang, S. Lodha, S. Rajan, *Appl. Phys. Lett.* **2017**, 111, 023502.
- [37] K. Nomura, K. Goto, R. Togashi, H. Murakami, Y. Kumagai, A. Kuramata, S. Yamakoshi, A. Koukitu, *J. Cryst. Growth* **2014**, 405, 19.
- [38] H. Murakami, K. Nomura, K. Goto, K. Sasaki, K. Kawara, Q. T. Thieu, R. Togashi, Y. Kumagai, M. Higashiwaki, A. Kuramata, S. Yamakoshi, B. Monemar, A. Koukitu, *Appl. Phys. Express* **2015**, 8, 015503.
- [39] K. Goto, K. Konishi, H. Murakami, Y. Kumagai, B. Monemar, M. Higashiwaki, A. Kuramata, S. Yamakoshi, *Thin Solid Films* **2018**, 666, 182.
- [40] Y. Zhang, F. Alema, A. Mauze, O. S. Koksaldi, R. Miller, A. Osinsky, J. S. Speck, *APL Mater.* **2019**, 7, 022506.
- [41] Z. Feng, A. F. M. A. U. Bhuiyan, M. R. Karim, H. Zhao, *Appl. Phys. Lett.* **2019**, 114, 250601.
- [42] F. Alema, Y. Zhang, A. Osinsky, N. Valente, A. Mauze, T. Itoh, J. S. Speck, *APL Mater.* **2019**, 7, 121110.
- [43] M. J. Tadjer, F. Alema, A. Osinsky, M. A. Mastro, N. Nepal, J. M. Woodward, R. L. Myers-Ward, E. R. Glaser, J. A. Freitas, A. G. Jacobs, J. C. Gallagher, A. L. Mock, D. J. Pennachio, J. Hajzus, M. Ebrish, T. J. Anderson, K. D. Hobart, J. K. Hite, C. R. Eddy, *J. Phys. D* **2021**, 54, 034005.
- [44] A. F. M. A. U. Bhuiyan, Z. Feng, J. M. Johnson, Z. Chen, H.-L. Huang, J. Hwang, H. Zhao, *Appl. Phys. Lett.* **2019**, 115, 120602.
- [45] P. Ranga, A. Bhattacharyya, A. Rishinaramangalam, Y. K. Ooi, M. A. Scarpulla, D. Feezell, S. Krishnamoorthy, *Appl. Phys. Express* **2020**, 13, 045501.
- [46] M. Higashiwaki, K. Konishi, K. Sasaki, K. Goto, K. Nomura, Q. T. Thieu, R. Togashi, H. Murakami, Y. Kumagai, B. Monemar, A. Koukitu, A. Kuramata, S. Yamakoshi, *Appl. Phys. Lett.* **2016**, 108, 133503.
- [47] K. Konishi, K. Goto, H. Murakami, Y. Kumagai, A. Kuramata, S. Yamakoshi, M. Higashiwaki, *Appl. Phys. Lett.* **2017**, 110, 103506.
- [48] C.-H. Lin, Y. Yuda, M. H. Wong, M. Sato, N. Takekawa, K. Konishi, T. Watahiki, M. Yamamuka, H. Murakami, Y. Kumagai, M. Higashiwaki, *IEEE Electron Device Lett.* **2019**, 40, 1487.
- [49] W. Li, Z. Hu, K. Nomoto, R. Jinno, Z. Zhang, T. Q. Tu, K. Sasaki, A. Kuramata, D. Jena, H. G. Xing, in *2018 IEEE Int. Electron Devices Meeting (IEDM)*, IEEE, Piscataway, NJ, USA **2018**, <https://doi.org/10.1109/IEDM.2018.8614693>.
- [50] W. Li, K. Nomoto, Z. Hu, D. Jena, H. G. Xing, *Appl. Phys. Express* **2019**, 12, 061007.

- [51] T. Watahiki, Y. Yuda, A. Furukawa, M. Yamamuka, Y. Takiguchi, S. Miyajima, *Appl. Phys. Lett.* **2017**, 111, 222104.
- [52] X. Lu, X. Zhou, H. Jiang, K. W. Ng, Z. Chen, Y. Pei, K. M. Lau, G. Wang, *IEEE Electron Device Lett.* **2020**, 41, 449.
- [53] H. H. Gong, X. H. Chen, Y. Xu, F.-F. Ren, S. L. Gu, J. D. Ye, *Appl. Phys. Lett.* **2020**, 117, 022104.
- [54] N. Allen, M. Xiao, X. Yan, K. Sasaki, M. J. Tadjer, J. Ma, R. Zhang, H. Wang, Y. Zhang, *IEEE Electron Device Lett.* **2019**, 40, 1399.
- [55] Z. Hu, Y. Lv, C. Zhao, Q. Feng, Z. Feng, K. Dang, X. Tian, Y. Zhang, J. Ning, H. Zhou, X. Kang, J. Zhang, Y. Hao, *IEEE Electron Device Lett.* **2020**, 41, 441.
- [56] Y. Zhang, J. Zhang, Z. Feng, Z. Hu, J. Chen, K. Dang, Q. Yan, P. Dong, H. Zhou, Y. Hao, *IEEE Trans. Electron Devices* **2020**, 67, 3948.
- [57] M. Higashiwaki, K. Sasaki, A. Kuramata, T. Masui, S. Yamakoshi, *Appl. Phys. Lett.* **2012**, 100, 013504.
- [58] K. Sasaki, M. Higashiwaki, A. Kuramata, T. Masui, S. Yamakoshi, *Appl. Phys. Express* **2013**, 6, 086502.
- [59] T. Kamimura, K. Sasaki, M. H. Wong, D. Krishnamurthy, A. Kuramata, T. Masui, S. Yamakoshi, M. Higashiwaki, *Appl. Phys. Lett.* **2014**, 104, 192104.
- [60] M. Higashiwaki, K. Sasaki, T. Kamimura, M. H. Wong, D. Krishnamurthy, A. Kuramata, T. Masui, S. Yamakoshi, *Appl. Phys. Lett.* **2013**, 103, 123511.
- [61] M. Higashiwaki, K. Sasaki, M. H. Wong, T. Kamimura, D. Krishnamurthy, A. Kuramata, T. Masui, S. Yamakoshi, in *2013 IEEE International Electron Devices Meeting*, IEEE, Piscataway, NJ, USA **2013**, <https://doi.org/10.1109/IEDM.2013.6724713>.
- [62] M. H. Wong, K. Sasaki, A. Kuramata, S. Yamakoshi, M. Higashiwaki, *IEEE Electron Device Lett.* **2016**, 37, 212.
- [63] M. H. Wong, A. Takeyama, T. Makino, T. Ohshima, K. Sasaki, A. Kuramata, S. Yamakoshi, M. Higashiwaki, *Appl. Phys. Lett.* **2018**, 112, 023503.
- [64] T. Kamimura, Y. Nakata, M. Higashiwaki, *Appl. Phys. Lett.* **2020**, 117, 253501.
- [65] K. D. Chabak, D. E. Walker, A. J. Green, A. Crespo, M. Lindquist, K. Leedy, S. Tetlak, R. Gilbert, N. A. Moser, G. Jessen, in *2018 IEEE MTT-S Int. Microwave Workshop Series on Advanced Materials and Processes for RF and THz Applications (IMWS-AMP)*, IEEE, Piscataway, NJ, USA **2018**, <https://10.1109/IMWS-AMP.2018.8457153>.
- [66] Z. Xia, H. Xue, C. Joishi, J. McGlone, N. K. Kalarickal, S. H. Sohler, M. Brenner, A. Arehart, S. Ringel, S. Lodha, W. Lu, S. Rajan, *IEEE Electron Device Lett.* **2019**, 40, 1052.
- [67] M. H. Wong, K. Goto, H. Murakami, Y. Kumagai, M. Higashiwaki, *IEEE Electron Device Lett.* **2019**, 40, 431.
- [68] M. H. Wong, C.-H. Lin, A. Kuramata, S. Yamakoshi, H. Murakami, Y. Kumagai, M. Higashiwaki, *Appl. Phys. Lett.* **2018**, 113, 102103.
- [69] M. H. Wong, H. Murakami, Y. Kumagai, M. Higashiwaki, *IEEE Electron Device Lett.* **2020**, 41, 296.
- [70] W. Li, K. Nomoto, Z. Hu, T. Nakamura, D. Jena, H. G. Xing, in *2019 IEEE Int. Electron Devices Meeting (IEDM)*, IEEE, Piscataway, NJ, USA **2019**, <https://doi.org/10.1109/IEDM19573.2019.8993526>.



Masataka Higashiwaki received his B.S., M.S., and Ph.D. in solid-state physics from Osaka University, Japan, in 1994, 1996, and 1998, respectively. After a 2-year postdoctoral fellowship, in 2000, he joined Communications Research Laboratory (CRL), Japan. From 2007 to 2010, he took temporary leave from National Institute of Information and Communications Technology (NICT), which was renamed from CRL, and joined Department of Electrical and Computer Engineering, University of California, Santa Barbara, as a project scientist. He returned to NICT in 2010 and started pioneering work on Ga₂O₃-based electronics. His expertise is in compound semiconductor devices and materials.